

# Multichannel Image Segmentation Algorithm for Agricultural Crop Detection

Anna Denisova, Andrey Kuznetsov, Nikolay Glumov

Samara National Research University  
34, Moskovskoe shosse, Samara, 443086, Russian Federation  
<http://www.ssau.ru>

**Abstract.** In this article we propose an algorithm for multichannel image segmentation within the predefined region of interest. The algorithm allows to determine whether the region of interest is homogeneous or not and it also produces a partition of the region of interest into homogeneous subsets and refines objects borders. The proposed method has been applied to remote sensing images of agricultural fields as a preliminary step of crop detection mechanism. Segmentation quality has been estimated by means of a specific measure proposed in this article.

## 1 Introduction

There are a lot of applications that require automatic segmentation to be performed as initial step [1]. For example, in the case of automatic crop detection on remote sensing images the initial agricultural field borders usually correspond to particular farmers field with several planted crops. To define areas occupied by each crop an automatic segmentation should be performed. Then the recognition process can be carried out as well as vegetation stages and planting conditions are determined. Another potential use of automatic segmentation in agriculture is acreage control. Often farmers do not trace all the processing steps for each field and a particular worker may slightly digress borders while sowing the plants. So that automatic segmentation technique might be able to assist farmers to control acreage independently using remote sensing data.

Existing image segmentation methods can be regarded in the scope of further classification of popular segmentation techniques given in [2]. Edge-based segmentation applies contour detection [3] [4]. For remote sensing images, it is supplementary mechanism because the most important information lies in color and texture properties of the objects. It is rather difficult to apply edge-based segmentation to any natural object because of the complex border form. Region-based segmentation [4] includes different clustering techniques on the first step and then produce segmentation by means of homogeneity functional optimization. These algorithms usually exploit only texture features and they are essentially pixel based methods. Due to the per pixel character of segmentation, it is more probable to achieve tiny over segmented contours on the final stage. More reliable segmentation methods correspond to per-field and multi-resolution segmentation [5]. For the first of them, it is assumed that initial object borders

are known and they can assist the segmentation. The latter analyzes image in different scales simultaneously. The key idea behind the multi-scale approach is to take into account properties of data with different resolution. There are some segmentation algorithms which use neural networks [6],[7]. The common disadvantage of neural network algorithms is huge training data set that must represent all possible variety of data. It is a big challenge to create such data set for any particular case. Therefore, the methods based on neural networks are not flexible in terms of novel types of data and features and could not be applied for internal borders refinement of the particular object.

In our article we assume that the database of objects' contours is available. This database may be presented in the form of vector map from geoinformation system (GIS). We explore the case of automatic analysis of internal map object structure and its border refinement, thus we consider only the explored object and its surroundings as input data. The aim of the segmentation in our case is to define significant object's parts that differ from each other by their spectral-spatial characteristics, i.e. to clarify an internal object structure. Resulting contours should separate an initial object into meaningful parts. The outside object border is supposed to be known from the vector map and is referred as the region of interest (ROI). It is assumed that multiple features are available.

As far as we suppose that it is more important to identify borders inside the ROI rather than to refine its contour, we have based our algorithm on a merge approach [8]. This approach includes two stages i.e. splitting the image into numerous tiny locally homogeneous areas and their merging into more complicated ones. As a result, the outside ROI contour will be initially presented with the precision of tiny homogeneous regions and the inside borders will be defined with the precision of the merging rule.

Managing the splitting and merging process allows our algorithm to work adaptively with each particular contrast and texture, which is highly determined by image resolution. Such opportunity is very important for the agricultural fields, because usually images are very different not only in sense of planted crops but also as a result of relief and image acquisition properties. Relief changes lead to texture variations within the fields with the same crop class. And acquisition parameters significantly determine particular image contrast properties.

The proposed algorithm has been revised by means of segmentation quality measure on the set of remote sensing images. Experiments have shown successful results in most of the cases and the best pair of the algorithm parameters has been recommended.

The article includes three main parts: problem statement, algorithm description and experimental evaluation of the method on remote sensing images. The article ends with conclusions and acknowledgements sections.

## 2 Problem statement

In our notations initial image of  $L$  features with size  $N_1 \times N_2$  is denoted by symbol  $X_l(n_1, n_2)$ ,  $0 \leq n_1 \leq N_1 - 1$ ,  $0 \leq n_2 \leq N_2 - 1$ ,  $0 \leq l \leq L - 1$ , where  $n_1$

and  $n_2$  are the coordinates of image pixel. The general segmentation problem is formulated as optimization problem:

$$S = \{S_k\}, 0 \leq k \leq K_S - 1, \Omega = \{\Omega_i\}, 0 \leq i \leq K_\Omega - 1, \bigcup_k S_k \subset \Omega, \quad (1)$$

$$Q(S, \Omega) \mapsto \max. \quad (2)$$

where  $Q(S)$  is the segmentation quality measure,  $S = \{S_k\}, 0 \leq k \leq K_S - 1$  is a set of pixel subsets defining the results of segmentation,  $K_S$  is the number of subsets,  $\Omega = \{\Omega_i\}, 0 \leq i \leq K_\Omega - 1$  is an ideal segmentation and  $K_\Omega$  is ideal number of subsets.

We offer the following measure segmentation quality evaluation:

$$Q(S, \Omega) = \frac{1}{2} \left( \frac{1}{K_S} \sum_k \frac{\max_i |\Omega_i \cap S_k|}{|S_k|} + \frac{1}{K_\Omega} \sum_i \frac{\max_k |\Omega_i \cap S_k|}{|\Omega_i|} \right), \quad (3)$$

where  $|\dots|$  is the number of pixels per subset. The segmentation quality measure is based on the quantities introduced in [9]. It takes values from 0.5 to 1. The lower bound is achieved when one of the values  $K_S$  or  $K_\Omega$  is equal to one and the other is total number of image pixels. The upper bound of  $Q$  corresponds to the precise segmentation.

### 3 Algorithm description

Let us denote the source remote sensing image as  $F_m(n_1, n_2), 0 \leq m \leq M - 1, 0 \leq n_1 \leq N_1 - 1, 0 \leq n_2 \leq N_2 - 1$ . Here by we describe all of the processing steps of our algorithm including preprocessing and feature calculation.

Step 1. Input data preparation.

We clip initial remote sensing image within the bounding box of vector map object to be analyzed using standard GIS instruments. The resulting piece of the image represents the region of interest and contains all pixels corresponding to analyzed object and its surroundings.

Step 2. Feature extraction.

This stage includes calculation of initial feature image  $X_l(n_1, n_2), 0 \leq n_1 \leq N_1 - 1, 0 \leq n_2 \leq N_2 - 1, 0 \leq l \leq L - 1$  using local averages and variations for each pixel block with  $W \times W$  size in the source image. The number of features  $L = 2M$  is two times higher than the original image channel count, because these features are computed separately per each image component.

Step 3. Feature variance normalization.

To exclude the impact of different dynamic ranges for the computed features we normalize each component using its global standard deviation  $\sigma_l$ :

$$x_l(n_1, n_2) = \frac{X_l(n_1, n_2)}{\sigma_l}. \quad (4)$$

Step 4. Splitting image into tiny regions.

4.1. Before splitting initial image with segment indexes  $I(n_1, n_2)$ ,  $0 \leq n_1 \leq N_1, 0 \leq n_2 \leq N_2$  is initialized by zero:  $I(n_1, n_2)$ . Current number of segments is set to zero  $S = 0$  too. Further analysis is produced for the sequence of grids defined by shifting parameter  $a = 1$ ;

4.2. For each feature vector in the grid  $x(n_1, n_2), (n_1, n_2) \in T$  with step  $aW$ :

$$T = \{(n_1, n_2) : n_1 \bmod aW = 0, n_2 \bmod aW = 0\}, \quad (5)$$

where  $\bmod$  is the remainder after division, the neighborhood is determined. This neighborhood contains pixels located at distance  $aW$  per each spatial coordinate from the current pixel. There are three possible cases. First case is when the neighborhood pixels have different indexes of segments. Second case is when only one pixel has non zero segment index  $s$  for the current neighborhood. And the last case is when  $aW = 1$  and all neighborhood pixels have the same index  $s$ . If the second and third situations take place, then the condition of the similarity between feature vectors is checked:

$$\rho(x(n_1, n_2), x(n_1 \pm aW, n_2 \pm aW)) < \varepsilon, (n_1, n_2) \in T \quad (6)$$

where  $\rho$  is some distance metric i.e. Euclidean distance. If the condition (6) is fulfilled, the segment index  $I(n_1, n_2)$  is set to  $s$ . Otherwise, it is assigned to  $s_{max} + 1$ , where  $s_{max}$  is the biggest segment index at the current time.

In the first case, when there are several different values of segment index in the neighbourhood, current feature vector have to be compared with an average feature vectors for each of the presented segments:

$$\rho(x(n_1, n_2), E(s)) < \varepsilon, (n_1, n_2) \in T, \quad (7)$$

$$s = \operatorname{argmin}_{s \in \{I(n_1 \pm aW, n_2 \pm aW)\}} \rho(x(n_1, n_2), E(s)) \quad (8)$$

where  $E(s)$  is an average feature vector for the segment with index  $s$ . If this condition is fulfilled for some index  $s$ , it is stored in  $I(n_1, n_2)$  as a current estimate of the segment number.

4.3 The grid step is decreased in twice  $a = \frac{a}{2}$  and the steps from 4.1 to 4.3 are repeated while the condition  $aW \geq 1$  is valid.

Step 5. Merging.

For each pair of the adjacent segments two segments are merged if their average feature vectors are closer than the threshold value:

$$\rho(E(s_1), E(s_2)) < \varepsilon \quad (9)$$

Step 6. ROI border refinement.

This step is intended to the analysis of non zero points on the segment border. This analysis includes three steps listed below:

6.1 Distance map calculation for each feature vector. This map contains the distances  $\rho$  between current feature vector and average feature vectors of the segments corresponding to pixels within the local window  $W \times W$ .



6.2 Parabolic filtering of the distance map. Each value of the distance  $\rho$  within the window is multiplied by the coefficients of parabolic filter with same size  $W \times W$  and then the minimum is used as a result of filtration for current window position. The coefficients of parabolic filter are defined by following equation:

$$P(w_1, w_2) = w_1 * w_1 + w_2 * w_2, \quad (10)$$

where  $w_1$  and  $w_2$  take values from the range  $[-\frac{W}{2}, \frac{W}{2}]$ .

6.3 Final index of the segment is defined as the index of segment with the minimum filtered distance which is also less than  $\varepsilon$ .

The algorithm produces an image with the segments' indexes. Step 2 can be modified if it is necessary to apply any other features.

## 4 Experimental evaluation

The proposed algorithm has been used for agricultural fields analysis. Input images were acquired by sensor UK DMC for the Samara region. Image resolution was 22 meters per pixel. Test images were obtained during the period from the 1st of April 2012 till the 15th of June.

The aim of our experimental research was to define which parameter values deliver the best method performance. The following groups of factors may significantly affect segmentation quality. The first group accumulates images which are partially clouded and with shadows from the clouds. For these images clouds and shadows always are distinguished as different segments and leads to over segmentation. This is irremovable error, therefore only cloudless images should be used. The second group accumulated images of fields with the rough relief structure. If there are some ditches, channels, ravines or the slope and curvature is high, it would be difficult to make segmentation properly. The last group includes rough-textured fields. Usually, non hybrid field has the rough texture of its surface because of the agricultural management events. In this case there can be regular lines or spots on the images inside the borders of the field. If the texture elements are enough big, they may lead to over segmentation too. Thus, the results of the algorithm are highly dependent on input data and can not be applied without calibration.

For the agricultural field border monitoring we have used infrared, red and green spectral channels. The features were local averages and variances for each spectral channel.

We have used a sample set of 120 images for the typical problem cases listed above (30 images per category) and 30 images with simple non hybrid structure (as an example of the case of good conditions for the algorithm). The ideal segmentation has been done manually. The examples of test images are presented in fig. 1.

The quality of segmentation for each image has been estimated by means of  $Q$  criterion described above. We have tested algorithm parameters for the

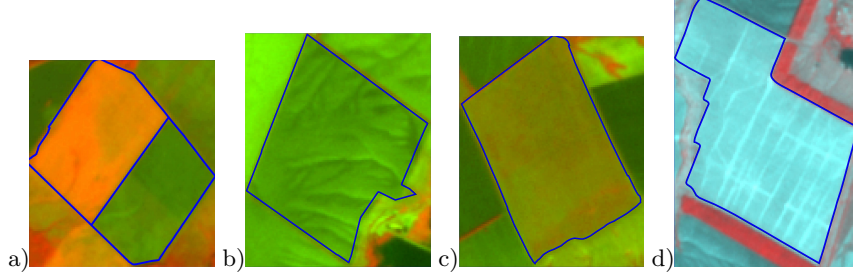


**Fig. 1.** The examples of test images for different categories a) hybrid field, b) non hybrid field with complex relief, c) simple non hybrid field, d) textured non hybrid field. Blue border is an ideal segmentation contour.

following ranges: for  $\varepsilon$  from 0.1 to 2 with step 0.1, for  $W$  from 3 to 15 with step 2.

To inspect the relationship between each category and quality of segmentation we have assigned the index  $g$  to each of the four image categories:  $g = 1$  for hybrid field,  $g = 2$  for non hybrid field with complex relief,  $g = 3$  for simple non hybrid field,  $g = 4$  for textured hybrid field. Image index in the particular group is denoted as  $j$  and there are  $J = 30$  images per each category.

For all pairs of parameters  $W$  and  $\varepsilon$  an averages and variances of  $Q$  per group and for the whole image set have been calculated using formulas:

$$m_{Qg}(W, \varepsilon) = \frac{1}{J} \sum_{j=1}^J Q_{gj}(W, \varepsilon), \quad (11)$$

$$\sigma_{Qg}(W, \varepsilon) = \sqrt{\frac{1}{J} \sum_{j=1}^J (Q_{gj}(W, \varepsilon) - m_{Qg}(W, \varepsilon))^2}, \quad (12)$$

$$m_Q(W, \varepsilon) = \frac{1}{GJ} \sum_{g=1}^G \sum_{j=1}^J Q_{gj}(W, \varepsilon), \quad (13)$$

$$\sigma_Q(W, \varepsilon) = \sqrt{\frac{1}{GJ} \sum_{g=1}^G \sum_{j=1}^J (Q_{gj}(W, \varepsilon) - m_Q(W, \varepsilon))^2}. \quad (14)$$

For each category we have selected an optimal pair of parameters  $P_{optg}$  as a pair that fulfill the following condition:

$$P_{optg} = \{(W, \varepsilon) : m_{Qg}(W, \varepsilon) \geq m_g - \sigma_g\}, \quad (15)$$

where

$$m_g = \max_{(W, \varepsilon)} [m_{Qg}(W, \varepsilon)],$$

$$\sigma_g = \max_{(W, \varepsilon) \in P_g} [\sigma_{Qg}(W, \varepsilon)],$$

$$P_g = \{(W, \varepsilon) : m_{Qg}(W, \varepsilon) = m_g\}.$$

The table of  $m_g$  and  $\sigma_g$  values for each category is shown below.

**Table 1.**  $m_g$  and  $\sigma_g$  values for each image category

Category	$g$	$m_g$	$\sigma_g$
hybrid field	1	0.945	0.031
non hybrid field with complex relief	2	0.990	0.012
simple non hybrid field	3	0.986	0.014
textured hybrid field	4	0.989	0.007

The optimal pairs of the parameters for the whole image set have been found as intersection of optimal parameters sets for each category  $P_{optg}$ .

The table 2 contains optimal for the whole sample set parameters and average segmentation quality measure  $m_Q(W, \varepsilon)$  for them.  $m_{Q_1}(W, \varepsilon)$  is an average value of the segmentation quality measure only for the hybrid field samples.

**Table 2.** Optimal pairs of parameters

$W$	$\varepsilon$	$m_Q(W, \varepsilon)$	$m_{Q_1}(W, \varepsilon)$
5	0.5	0.969	0.931
5	0.6	0.971	0.931
5	0.8	0.967	0.914

Fig. 2 illustrates the segmentation results with the best pair of parameters  $W = 5$  and  $\varepsilon = 0.6$  for the images from the fig. 1.

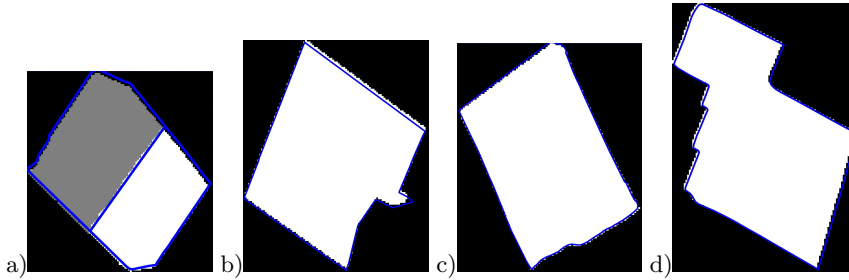


**Fig. 2.** Segmentation results with the best pair of parameters  $W = 5$  and  $\varepsilon = 0.6$  for the images from the fig. 1

## 5 Conclusion

In this article, we have proposed an algorithm that helps to make a segmentation of particular objects. It is based on two steps: excess segmentation and merging. The quality of segmentation depends on the similarity threshold and initial degree of over segmentation that is controlled by the window size. Algorithm has been tested on agricultural field images and the best pair of parameters have been selected. The control parameters of the algorithm allow to use it for another kind of data with different resolution and contrast properties, but the calibration must be carried out in advance.

**Acknowledgements** This study was financially supported by RFBR projects 16-37-00043 mola, 16-29-09494 ofim.

## References

1. Narkhede, H.P.: Review of image segmentation techniques. *International Journal of Science and Modern Engineering*. 1(8), 54–61 (2013)
2. Blaschke, T., et al.: Object-oriented image processing in an integrated GIS remote sensing environment and perspectives for environmental applications. *Environmental information for planning, politics and the public*. 2, 555–570. (2000)
3. Rydberg, A., Borgefors, G.: Integrated method for boundary delineation of agricultural fields in multispectral satellite images. *IEEE Transactions on Geoscience and Remote Sensing*. 39(11), 2514–2520. (2001)
4. Mueller, M., Segl, K., Kaufmann, H.: Edge-and region-based segmentation technique for the extraction of large, man-made objects in high-resolution satellite imagery. *Pattern recognition*. 37(8), 1619–1628. (2004)
5. Blaschke, T., Burnett, C., Pekkarinen, A.: Image segmentation methods for object-based analysis and classification. *Remote sensing image analysis: Including the spatial domain*. 211–236. (2006)
6. Basu, S., Ganguly, S., Mukhopadhyay, S.: DeepSat A Learning framework for Satellite Imagery. *Proceedings of the 23rd SIGSPATIAL International Conference on Advances in Geographic Information Systems*. (2015)
7. Chen, L.-C., Papandreou, G., Kokkinos, I., Murphy, K., Yuille, A.L.: DeepLab: Semantic Image Segmentation with Deep Convolutional Nets, Atrous Convolution, and Fully Connected CRFs. *Proceedings of the 23rd SIGSPATIAL International Conference on Advances in Geographic Information Systems*. (2015)
8. Sonka, M., Hlavac, V., Boyle, R.: *Image processing, analysis, and machine vision*. *IEEE Transactions on Geoscience and Remote Sensing*. Cengage Learning. (2014)
9. Weidner, U.: Contribution to the assessment of segmentation quality for remote sensing applications. *International Archives of Photogrammetry, Remote Sensing and Spatial Information Sciences*. 37(B7), 479–484. (2008)